Fiber Formation from Silk Fibroin Using Pressurized Gyration

*Phoebe Louiseanne Heseltine, Joseph Hosken, Chris Agboh, David Farrar, Shervanthi Homer-Vanniasinkam, and Mohan Edirisinghe**

Silk has attracted considerable interest for use in biomedical applications due to its high strength and promising biocompatibility. Degummed silk, consisting only of silk fibroin (SF), has been processed using various methods and can be made into films, sponges, and fibers. Pressurized gyration (PG) is capable of rapidly producing aligned fibers and offers a great amount of control over their structure and morphology. Here, SF fibers are produced for the first time using PG. The effect of varying SF concentration and applied working pressure to the gyration vessel is reported, along with the resulting effect on fiber diameter, morphology, and structural composition. Aligned microfibers are found at concentrations of 8, 10, 12 w/v%, with the lowest fiber diameters reported at 8 w/v% SF 0.3 MPa applied pressure (2.1 ± 1.3 µm). Fourier-transform infrared spectroscopy (FTIR) confirms the existence of PG spun fibers in both random coil and β-sheet formations.

Fibers in the nano- to micrometer range are an exciting class of material with an ever-expanding portfolio of applications. Their unique physicochemical properties such as high specific surface area to volume ratio, tailorable surface morphology and porosity, and their ability to be functionalized for a specific end use, make them powerful tools for use in research and

P. L. Heseltine, J. Hosken, Prof. S. Homer-Vanniasinkam,
Prof. M. Edirisinghe
Department of Mechanical Engineering
University College London
Torrington Place, London WC1E 7JE, UK
E-mail: m.edirisinghe@ucl.ac.uk
Dr. C. Agboh, D. Farrar
Xiros Ltd., Springfield House, White House Lane
Leeds LS19 7UE, UK
Prof. S. Homer-Vanniasinkam
Leeds Vascular Institute
Leeds General Infirmary
Great George Street, Leeds LS1 3EX, UK
Prof. S. Homer-Vanniasinkam
Division of Surgery
University of Warwick & University Hospitals Coventry
and Warwickshire NHS Trust
Clifford Bridge Rd, Coventry CV2 2DX, UK

The ORCID identification number(s) for the author(s) of this article
can be found under https://doi.org/10.1002/mame.201800577.

manufacturing.[1–3] Polymer fibers have been used extensively in energy storage, filtration, automotive industries, sensing, and as biomaterials—for example, in tissue engineering and drug delivery.[4–9]

For fabrication of fibers, several methods have been employed such as self-assembly, phase separation, template-assisted synthesis, centrifugal spinning, and melt-blowing, yet most of these methods are limited by low production rates.[10–13] For example, although self-assembly allows for the production of fine fibers, it is a time-consuming process. Phase separation has shown promise, however only some polymers can be used in this process. Electrospinning has become popular due to the amount of control that it allows in fiber formation in terms of their uniformity and length. Essentially, this method uses an electric field to drive the formation of a polymer fiber jet between a charged nozzle and a collector.[14] Contemplating these advantages, through varying technical parameters such as solution electrical conductivity, collector distance, solution viscosity, flow rate, and concentration, fibers can be spun. However, electrospinning is limited by its requirement for the use of polar solvents which restricts the range of polymers that can be used. Not only this, it normally requires a needle and tubing which can become easily clogged. Finally, electrospinning operates in a random whipping motion, greatly affecting the morphology and deposition of the fibers produced.[15]

In recent years, centrifugal spinning has been utilized as a needle-free method of fiber fabrication that relies on the centrifugal force of a rotating spinning head to eject polymer solution from orifices on its walls. Centrifugal spinning typically achieves higher production rates than electrospinning and allows for spinning of charge-free polymeric systems. Five years ago, pressurized gyration (PG) was introduced as a versatile and convenient technique to prepare fibers in a one-step production method.[16] As with fiber formation from centrifugal spinning methods, PG utilizes a high rotational speed to spin fibers from a cylindrical vessel containing polymer solution, yet the co-application of working pressure offers an additional parameter by which fiber outcome can be controlled. The rotational speed can also be increased to further reduce fiber diameter.

Fiber generation using the PG system can be attributed to the combined effect of centrifugal and dynamic fluid flow forces that exceed the surface tension. It is the result of instability at the liquid–air interface that produces nanofibers, as the liquid

**ADVANCED
SCIENCE NEWS**

www.advancedsciencenews.com

**Macromolecular
Materials and Engineering**

www.mme-journal.de

is ejected from the orifices of the gyration vessel. The system is dependent on solvent properties such as evaporation rate and collector distance and when the jet is ejected from the orifices it solidifies to form fibers at the collector. To date, several known biocompatible polymers have been successfully spun into fibers using PG.[16]

Silk fibers in their natural state, extracted from *Bombyx mori* (silkworm) silk, are comprised of the proteins fibroin and sericin, whereby sericin is bound as a glue to the silk fibroin (SF) fibrils to form fibers.[17] Fibroin is the main structural component of silk and is a fibrous protein that is formed of two peptide chains of differing molecular weights, 25 kDa (light fraction) and 350 kDa (heavy fraction), which are linked by a disulfide bond.[18] In the *B. mori* silk gland fibroin has a random coil formation, yet once it is spun into fibers the structure changes to a semi-crystalline ß-sheet structure dispersed in an amorphous matrix.[19]

SF is a biodegradable and biocompatible material with promising applications in wound healing, tissue engineering, and drug delivery.[20–22] As a biomaterial, silk sutures have been used extensively since ancient times and are still used today.[23] SF is a naturally derived protein-based polymer with a history of use in US Food and Drug Administration approved devices. It is advantageous in that it can be easily chemically modified, exhibits good mechanical toughness, it is permeable to oxygen, water, carbon dioxide, and the degradation rate can be adjusted.[24–27] SF can be separated from sericin in a degumming process, allowing it to be used in biomedical applications, whereby the presence of sericin would cause an adverse immunological response.[28] The degummed SF is a versatile material, which can be processed into films, hydrogels, solvent-sponges, non-woven mats, aqueous sponges, meshes, and fibers.[29–35]

Regenerated SF fibers have been produced using centrifugal spinning and electrospinning but the effect of PG on their formation is unknown. To date, no fibers have been created using PG as a fiber forming method. In this communication, we aim to illustrate the results of fibers manufactured from PG. SF has the capacity to have improved polymer yield when processed using PG and the potential to exhibit alternate fiber networks.

The concentrations of SF that were used were selected based on preliminary work where it was found that below 6 w/v% there was insufficient chain entanglement within the solutions to lead to fiber formation. Hexafluoroisopropanol (HFIP) was chosen as a solvent due to its widely reported ability to dissolve SF.[19] Viscosity and surface tension are critical to fiber formation and depend on other polymer properties such as molecular weight, concentration, and interaction with solvent.[13] The measured values for surface tension and viscosity are recorded in **Table 1**. In this instance, it was found that both the viscosity and surface tension of the three silk solutions increased systematically with increasing SF concentration.

In PG, **Figure 1**a fiber formation occurs due to manipulation of the Rayleigh–Taylor instability of the polymer solution. As the gyration vessel spins, polymer solution is ejected from the orifices due to centrifugal force. There is a surface tension gradient along the liquid–air interface which results in separation of the polymer solution from the surrounding air. A Gibbs–Marangoni stress occurs that is tangential to the liquid–gas interface and the emerging polymer droplet undergoes stretching.[36] The jet is elongated due to the pressure difference

Table 1. Polymer solution properties, pressure, and mean fiber diameters achieved.

Concentration [w/v%]	Surface tension [mN m^{-1}]	Viscosity [mPa s]	Applied pressure [MPa]	Mean fiber diameter [µm]
8	30.5 ± 0.8	118.0 ± 2.6	0.1	4.0 ± 1.5
			0.2	3.2 ± 1.5
			0.3	2.1 ± 1.3
10	33.3 ± 0.6	160.9 ± 6.1	0.1	10.6 ± 2.3
			0.2	7.2 ± 2.4
			0.3	6.3 ± 2.6
12	35.5 ± 1.3	200.7 ± 2.8	0.1	15.7 ± 3.0
			0.2	23.3 ± 8.4
			0.3	29.6 ± 11.0

between the drum and the orifices and as the solvent evaporates, fiber thinning occurs.[37] Fibers are then deposited onto the walls of the collector (Figure 1b). The fibers that are regenerated into a finer network of microscale fibers after gyratory spinning are seen in Figure 1c.

The solutions were spun consecutively at 36 000 rpm in ambient conditions. Fibers were formed from all three solutions across the range of pressures, the diameters achieved are listed in Table 1. It was found that the lowest concentration used, 8 w/v%, produced systematically finer fibers and at a pressure of 0.3 MPa, the fiber diameter was lowest at 2.1 ± 1.3 µm. As the concentration increased, the fiber diameters increased and the largest fibers were produced at a concentration of 12 w/v% at 0.3 MPa, 29.6 ± 11.0 µm. Increased solution concentration results in thicker fibers as the level of polymer chain entanglement is increased, as is solution viscosity.[16] As demonstrated by Hong et al., in PG there must a critical minimum polymer concentration, Ce, to achieve the level of chain entanglement necessary in order to achieve fibers rather than beads or droplets.[38] In this instance, a greater level of SF in the solution increases the overlapping of SF chains, and thus leads to greater entanglement.

It was found that increasing the gas pressure greatly affected fiber diameter for all of the concentrations. For fibers at 8 and 10 w/v% there was a general decrease in fiber diameter with gas pressure. For fibers at 8 w/v%, the diameter decreased from 4.0 ± 1.5 µm at 0.1 MPa to 2.1 ± 1.3 µm at 0.3 MPa. Similarly, at a concentration of 10 w/v% fiber diameter decreased from 10.6 ± 2.3 µm at 0.1 MPa to 6.3 ± 2.6 µm at 0.3 MPa applied pressure. In PG, a pressure differential within the vessel results in acceleration of the polymer solution out from the orifices. Increased gas pressure causes jet elongation and therefore fiber thinning, hence normally thinner fibers are achieved at higher gas pressures—this is consistent with the literature.[37]

For fibers produced at a concentration of 12 w/v% the opposite effect is observed, fiber diameter increases from 15.7 ± 3.0 µm at 0.1 MPa to 29.6 ± 11.0 µm at 0.3 MPa applied pressure. This could be explained by the presence of an increased level of chain entanglement due to stronger molecular interactions arising from a higher concentration, having an effect on the flow of polymer solution out from the orifice leading to thick branching fiber networks (**Figure 2**g–i).
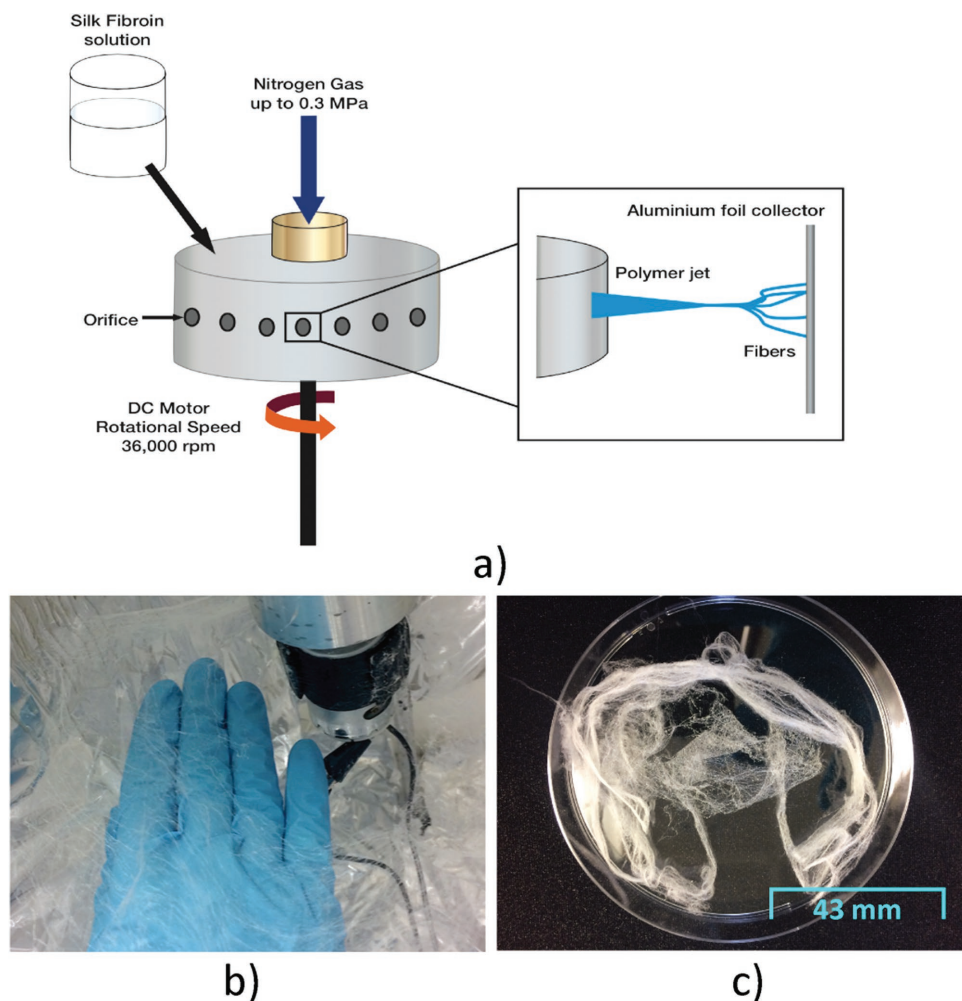
Figure 1. a) PG set-up, b) SF fibers deposited on the walls of PG set-up. c) SF processed using PG, 8 w/v% at 0.2 MPa pressure.

Both working pressure and solution concentration have a marked effect on fiber diameter distribution. For 8 w/v% concentration (Figure 2a–c), at 0.1 MPa pressure, the fibers appear smooth and somewhat aligned (Figure 2ai). Fiber diameter distribution for 8 w/v% is broad at 0.1 MPa pressure (Figure 2aii) yet becomes narrower for 0.2 MPa (Figure 2bii). Although a greater presence of beads is observed at 0.3 MPa (Figure 2ci), the majority of fibers at this pressure are in the range of 1–2 µm (Figure 2cii).

For 10 w/v% at 0.1 MPa pressure, smooth aligned fibers were observed (Figure 2di) with a fairly narrow diameter distribution (Figure 2dii). When the pressure was applied at 0.2 MPa there was an increased presence of beads, yet fibers were still aligned in appearance (Figure 2e). At 0.3 MPa, the fibers exhibited mainly beaded morphology, with branching fibers from larger sections of dried polymer solution (Figure 2fi). Aligned fibers are a typical result of PG, where the rotation of the drum and ejection of fibers is uniform as a result of the spinning vessel. A similar result can be achieved via other methods such as stable jet electrospinning, where an appropriate viscosity is reached and high voltage is applied to yield a stable jet. Addition of a rotating collector enhances the alignment.[39] Yi et al.

reported unidirectionally aligned fibers prepared from an SF/PEO spinning dope (mass ratio 88: 12), where the addition of high molecular weight PEO produced a stable linear jet, as viscosity was increased and solution conductivity was decreased.[40]

At the highest concentration of 12 w/v%, at 0.1 MPa pressure, fibers appeared indented and branched in their morphology, likely due to the separation of the primary jet into smaller jets (Figure 2gi). As a result, a broad distribution in fiber diameter was observed (Figure 2gii). Increasing the working pressure to 0.2 MPa yielded wide flat fibers with a depressed surface and ribbon-like morphology (Figure 2hi). This type of morphology can be attributed to the fast evaporation of the highly volatile HFIP solvent from the fiber surface, resulting in the fiber structure collapsing in the center.[41] An increase in working pressure to 0.3 MPa gave the broadest fiber diameter distribution (Figure 2i.ii), with a similar collapsed ribbon-like morphology of fibers to those produced at 0.2 MPa, except more branching structures were revealed as increased working pressure increased the rate of solvent evaporation even further (Figure 2i.i). At a given applied pressure and rotational speed (kept constant in this work), increase in silk concentration causes an increase in fiber diameter
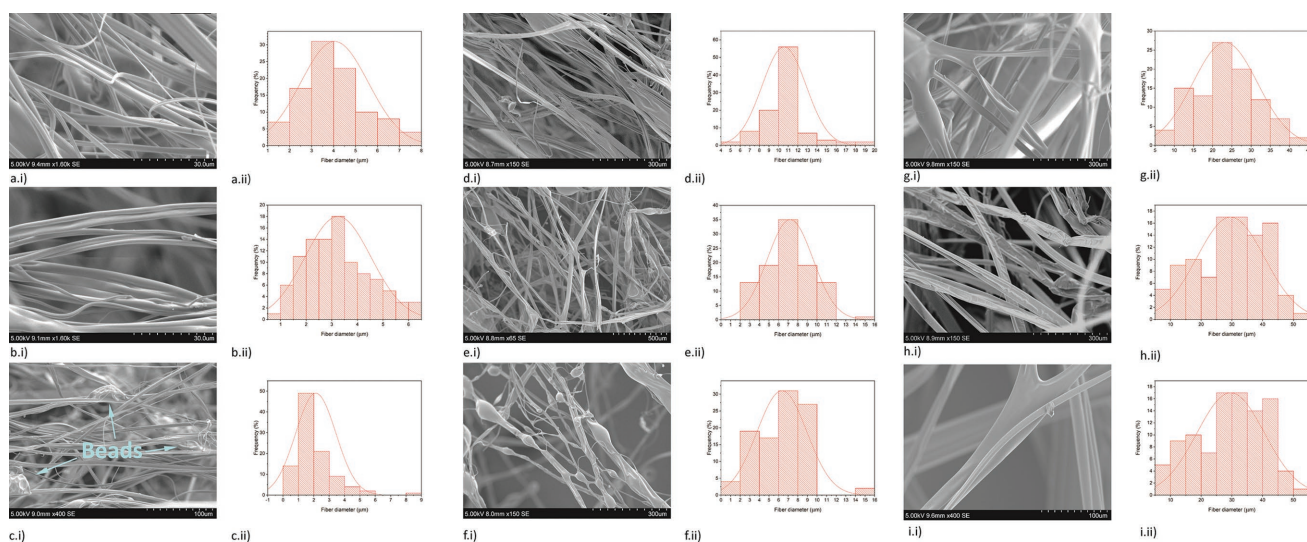
Figure 2. SEM images of 8 w/v% fibers at ai) 0.1, bi) 0.2, and ci) 0.3 MPa and aii, bii, cii) respective fiber diameter distributions. SEM images of 10 w/v% fibers at di) 0.1, ei) 0.2, and fi) 0.3 MPa and dii,eii,fii) respective fiber diameter distributions. SEM images of 12 w/v% fibers at gi) 0.1, hi) 0.2, and i.i) 0.3 MPa and gii, hii, i.ii) respective fiber diameter distributions—all spun at 36 000 rpm.

generated by PG. This is caused by increased viscosity, as illustrated in Table 1.

The magnitude of the applied gas pressure also has an effect on the yield of fibers. The yield was assessed qualitatively and defined as the total amount of fiber product ejected from the orifices of the vessel in 1 min of the drum rotating and pressure being applied. For concentrations of 8 and 10 w/v%, a general decrease in yield was observed as pressure was increased. In this work it was observed that at higher pressures, the polymer solution is scattered among the walls of the collector. As the motor accelerates to its maximum velocity, higher gas pressures cause rapid ejection of the solvent, resulting in a decreased amount of fiber deposition. At a concentration of 12 w/v%, an increase in fiber yield was found. This is likely due to have occurred as a result of thick branching fibers ejecting from the orifice at higher working pressures (Figure 2i.i). The highest mass achieved for these experiments was found at 12 w/v% at 0.2 MPa, whereby 76 mg of fiber was achieved after 30 s of spinning. Previous research has shown that PG is capable of producing high yields of polymeric fibers when compared to electrospinning and further quantitative experiments using SF will be conducted to confirm that this is indeed the case for this polymer.[16]

The surface topography of all SF fibers produced was pore free, as observed in **Figure 3**. Such fibers can be attributed to the

high-speed evaporation of HFIP solvent from the surface of the polymer jet.[42] The presence of collapsed fibers (Figure 3b,c) can be attributed to the thickness of the fiber achieved at higher concentrations and the effect of rapid solvent evaporation and subsequent diffusion of any remaining solvent through the surface of the fiber.[41] Porous fibers are often desirable for many applications, such as tissue engineering, to replicate the structure of the extracellular matrix. Porous SF fibers have been produced in electrospinning via the addition of porogens to the spinning dope. Ju et al. electrospun SF/PEO and applied sodium chloride nanocrystals to the collector. Fiber diameters were found to be in the range of 200 nm to 1.6 μm, while surface pores ranged from 0.5 to 3.5 μm. The addition of porogens to the tightly packed electrospun mat increased both mat thickness and porosity.[43]

SF fiber formation using PG has yielded a wide variety of morphological structures and varying fiber diameters, due to the effects of the solution properties of SF, as well as the varying gyration parameters. Fibers were generally found to be aligned and in the micrometer range, pore free, and with some beads-on-string morphology. This is similar to results observed by Liu et al. who conducted a comparative study of fibers produced both via electrospinning and centrifugal spinning using an SF concentration of 20 w/v% in formic acid.[44] They observed fiber diameters below 200 nm for electrospun
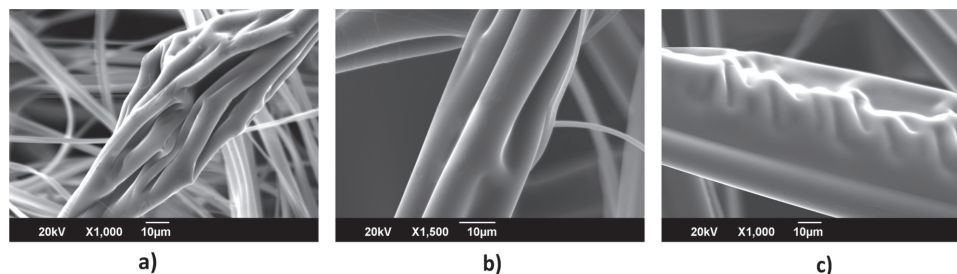

Figure 3. Fiber surface of a) 8 w/v% SF at 0.2 MPa, b) 10 w/v% SF at 0.2 MPa, c) 12 w/v% SF at 0.2 MPa.

1800577 (4 of 7)

**ADVANCED
SCIENCE NEWS**
www.advancedsciencenews.com

**Macromolecular
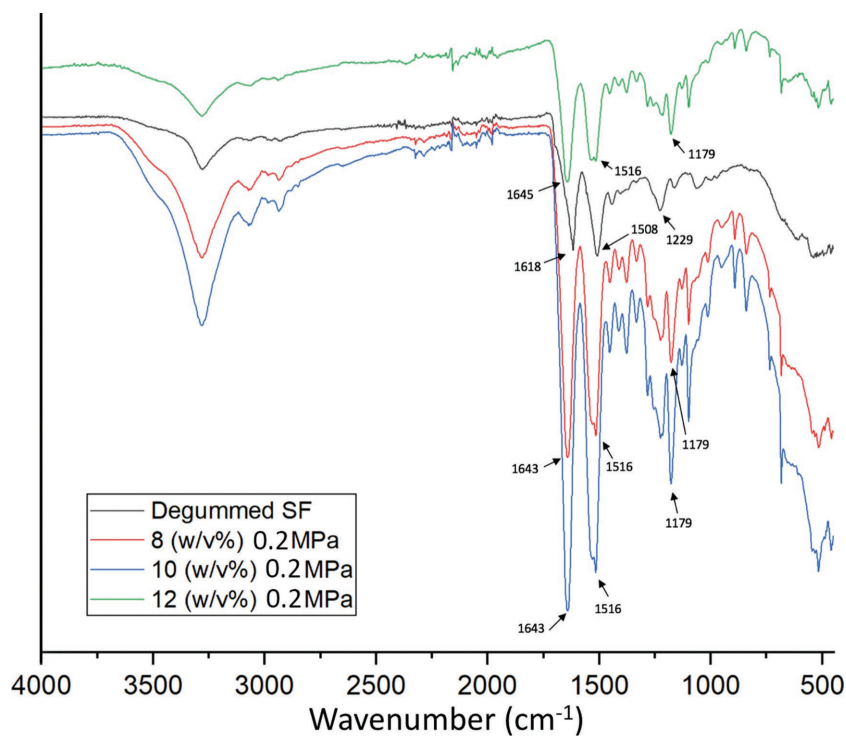Materials and Engineering**
www.mme-journal.de

Figure 4. FTIR spectra showing degummed SF, 8, 10, and 12 w/v%, all spun at an applied pressure of 0.2 MPa.

SF and at the same concentration, beaded fibers in the range of 400–2000 nm for centrifugally spun SF. Centrifugally spun fibers were found to be aligned, with thicker diameters, due to fast solvent evaporation due to air friction, which ultimately decreases the time of jet dragging and elongation—this is also true of fibers spun using PG. In the work of Liu et al.,[44] looser fiber mats were observed when SF was centrifugally spun, rather than electrospun, due to the absence of a charged collector. This is also true of PG, where fibers are deposited as the rotating drum spins and are accelerated by air flow through the application of pressure. In this study, higher solution concentration generally removed the beaded appearance from the fibers, yet also yielded greater fiber diameters. At 8 w/v%, the lowest diameters were achieved. Doping with other polymers such as PEO or PCL, as is popular with electrospinning, may improve solution properties and may allow for greater control over fiber outcome, including porosity. Nonetheless, PG offers a facile, one-step method of SF fiber production, whereby future modifications to both the spinning dope, forming parameters, and collection set-up will allow for refinement of the fiber outcome.

FTIR spectroscopy was used to verify the conformations of the degummed fibers prior to processing and after spinning into fibers using PG (**Figure 4**). The spectra of the SF fibers were characterized by transmittance bands. In all four transmittance spectra, the peptide backbone of amide I (C=O stretching) was present at 1618, 1643, 1643, and 1645 cm^{-1} for degummed SF, 8, 10, and 12 w/v%, respectively. Amide II (secondary N–H bending) was present at 1508, 1516, 1516, 1516 cm^{-1} in the same order. Amide III (C–N stretching) was present at 1229 cm^{-1} in degummed SF but was found at 1179 cm^{-1} for all of the fibers spun using PG. The positions of the bands

observed are indicative of the conformation of the SF fibers. For amide I, the degummed SF was likely present in ß-sheet conformation (absorption bands ≈1630 cm^{-1}), whereas for all of the PG spun fibers, the shift toward 1650 cm^{-1} is indicative of random coil.[45] For amide II, the absorption bands are all present around 1520 cm^{-1}, which indicates ß-sheet conformation. For amide III, ß-sheets are observed around 1270 cm^{-1}, whereas random coil is observed around 1230 cm^{-1}, thus indicating that both the degummed SF and PG spun SF exist in states somewhere between the two.[46] In this work, both the degummed SF and the PG spun SF exhibit typical random coil and ß-sheet conformation. It is known that the presence of stable ß-sheets is what provides enhanced mechanical strength, and one way of inducing this further would be through post-treatment of fibers with methanol.[47] The presence of ß-sheet conformation can be attributed to the shear stress that is applied to the polymer solution in fiber spinning through PG, similar to results observed by Liu et al. for centrifugally spun fibers.[48,44] Much like fiber formation within the *B. mori* silk gland, shear forces are exerted on the polymer solution as the vessel spins and gas pressure is applied. In higher concentrations, there are a greater number of fibroin chains, increasing the shearing forces applied to the polymer and thus leading to ß-sheet formation.

In this work, SF fibers in the microscale range have been successfully prepared for the first time using PG. Fiber diameters decreased as working pressure increases for concentrations of 8 and 10 w/v%, yet the opposite effect was observed for a concentration of 12 w/v%, suggesting a very fine range of SF solution properties from which fibers can be spun. It was also found that increasing concentration increased the average fiber diameter. SF fibers were found to be present both in random coil and in the ß-sheet conformation. PG offers a method of producing SF fibers with good control over fiber diameter and morphology. This novel method of preparing SF fibers can be optimized for use in many applications, for example, as an extracellular matrix for tissue engineering or for use in filtration applications. We also envisage preparation of SF nanofibers using PG.

Experimental Section

Materials: Raw *B. mori* silk fibers were obtained from E-Sarn (Thailand). The raw silk was degummed in a 0.033% sodium carbonate solution containing anionic and non-ionic detergents at a temperature of 90–100 °C for 30 min. Degummed fibers were given repeated rinses including hydroextraction before drying to constant weight (4-6) h in an oven at 105 °C. 1,1,1,3,3,3-Hexafluor-2-propanol (HFIP) was purchased from Sigma-Aldrich (Gillingham, UK).

Preparation of Bombyx mori Silk Fibroin Spinning Solution: The SF solutions were prepared by dissolving the degummed SF in HFIP. Solutions of 8, 10, 12 w/v % were used for this research. Each solution was prepared through addition of HFIP solvent to the degummed SF and then mechanically stirred for 48 h under ambient conditions. The

ADVANCED
SCIENCE NEWS
www.advancedsciencenews.com

Macromolecular
Materials and Engineering
www.mme-journal.de

solutions were subsequently processed into fibers using PG. SF requires "harsh" solvents in order to prepare processable solutions. HFIP was selected rather than other solvents such as formic acid, yet this is still not ideal. However, its high volatility ensures that there is less chance of residual HFIP in the fibers produced.

Fiber Formation Using Pressurized Gyration: A schematic of the PG set-up can be seen in Figure 1a. In this set-up, a rotating aluminum cylindrical vessel (60 mm in diameter × 35 mm high) was used with 24 perforations surrounding the core, each orifice had an internal diameter of 0.5 mm. The device radius was 30 mm with a wall thickness of 1 mm. For each of the prepared concentrations of SF, 5 mL of solution was loaded into the vessel, with the vessel lid screwed shut. Each concentration of SF solution was spun at 0.1, 0.2, and 0.3 MPa, all at an apparent speed of 36 000 rpm and at a collection distance of 120 mm, for approximately 30 s. Fibers were recovered from the walls of the collector once deposited onto aluminum sheeting. The ambient temperature was 19.5–22.6 °C. The relative humidity was 39.5–44.6%.

Solution Characterization: The changes in the solution viscosities with increasing concentration of SF were characterized using a programmable rheometer (DV-III Ultra, Brookfield Engineering Laboratories INC, Massachusetts, USA). Measurements of each solution were repeated three times, at a shear stress of approximately 5 Pa. The surface tensions of the solutions were also characterized using a tensiometer (Tensiometer K9, Kruss GmbH, Germany) and repeated five times to calculate the average.

Fiber Characterization

Scanning Electron Microscopy: Fibers formed from PG were examined using scanning electron microscopy (SEM). The samples were sputter coated twice with gold (Q150R ES, Quorum Technologies) for 3 min prior to imaging using SEM (Hitachi S-3400n). Mean fiber diameter was calculated using ImageJ software (NIH, Bethesda, Maryland, USA), whereby 100 fibers were measured at random. OriginPro software was then used to calculate the frequency distribution of the fibers.

Fourier Transform Infrared Spectroscopy: The infrared spectra of the fibers were recorded on a Perkin Elmer Spectrum-2 FTIR Spectrophotometer (PerkinElmer Inc., Beaconsfield, UK). The spectra of the fibers formed using PG were compared to that of the degummed SF provided by Xiros. Scans were taken in transmittance mode at an ambient temperature, between 4000 and 450 cm^{-1}. Four scans were taken with a resolution of 4 cm^{-1}. Spectra were analyzed using Essential FTIR software and OriginPro.

Conflict of Interest

The authors declare no conflict of interest.

[1] S. J. Eichhorn, W. W. Sampson, *J. R. Soc., Interface* **2010**, *7*, 641.
[2] D. Liang, B. S. Hsiao, B. Chu, *Adv. Drug Delivery Rev.* **2007**, *59*, 1392.
[3] R. E. Neisiany, S. N. Khorasani, M. Naeimirad, J. K. Y. Lee, S. Ramakrishna, *Macromol. Mater. Eng.* **2017**, *302*, 160055.
[4] S. Cavaliere, S. Subianto, I. Savych, D. J. Jones, J. Roziere, *Energy Environ. Sci.* **2011**, *4*, 4761.
[5] M. M. Zhu, J. Q. Han, F. Wang, W. Shao, R. H. Xiong, Q. L. Zhang, H. Pan, Y. Yang, S. K. Samal, F. Zhang, C. B. Huang, *Macromol. Mater. Eng.* **2017**, *302*, 16005353.
[6] R. Sood, S. Cavaliere, D. J. Jones, J. Roziere, *Nano Energy* **2016**, *26*, 729.
[7] G. R. Zhao, B. S. Huang, J. X. Zhang, A. C. Wang, K. L. Ren, Z. L. Wang, *Macromol. Mater. Eng.* **2017**, *302*, 1600476.
[8] R. Y. Basha, T. S. S. Kumar, M. Doble, *Macromol. Mater. Eng.* **2017**, *302*, 1600417.
[9] J. Ahmed, R. K. Matharu, T. Shams, U. E. Illangakoon, M. Edirisinghe, *Macromol. Mater. Eng.* **2018**, *303*, 1700577.
[10] P. Besenius, Y. Goedegebure, M. Driesse, M. Koay, P. H. H. Bomans, A. R. A. Palmans, P. Y. W. Dankers, E. W. Meijer, *Soft Matter* **2011**, *7*, 7980.
[11] J. D. Shao, C. Chen, Y. J. Wang, X. F. Chen, C. Du, *React. Funct. Polym.* **2012**, *72*, 765.
[12] C. R. Martin, *Science* **1994**, *266*, 1961.
[13] X. W. Zhang, Y. Lu, *Polym. Rev.* **2014**, *54*, 677.
[14] C. J. Luo, S. D. Stoyanov, E. Stride, E. Pelan, M. Edirisinghe, *Chem. Soc. Rev.* **2012**, *41*, 4708.
[15] L. Persano, A. Camposeo, C. Tekmen, D. Pisignano, *Macromol. Mater. Eng.* **2013**, *298*, 504.
[16] P. L. Heseltine, J. Ahmed, M. Edirisinghe, *Macromol. Mater. Eng.* **2018**, *303*, 1800218.
[17] J. Perez-Rigueiro, C. Viney, J. Llorca, M. Elices, *J. Appl. Polym. Sci.* **1998**, *70*, 2439.
[18] F. Vollrath, D. P. Knight, *Nature* **2001**, *410*, 541.
[19] K. A. Trabbic, P. Yager, *Macromolecules* **1998**, *31*, 462.
[20] W. Zhang, L. K. Chen, J. L. Chen, L. S. Wang, X. X. Gui, J. S. Ran, G. W. Xu, H. S. Zhao, M. F. Zeng, J. F. Ji, L. Qian, J. D. Zhou, H. W. Ouyang, X. H. Zou, *Adv. Healthcare Mater.* **2017**, *6*, 1700121.
[21] Z. H. Li, S. C. Ji, Y. Z. Wang, X. C. Shen, H. Liang, *Front. Mater. Sci.* **2013**, *7*, 237.
[22] M. A. Marin, R. R. Mallepally, M. A. McHugh, *J. Supercrit. Fluids* **2014**, *91*, 84.
[23] C. K. S. Pillai, C. P. Sharma, *J. Biomater. Appl.* **2010**, *25*, 291.
[24] S. Sofia, M. B. McCarthy, G. Gronowicz, D. L. Kaplan, *J. Biomed. Mater. Res.* **2001**, *54*, 139.
[25] B. B. Mandal, S. C. Kundu, *Acta Biomater.* **2010**, *6*, 360.
[26] L. S. Wray, X. Hu, J. Gallego, I. Georgakoudi, F. G. Omenetto, D. Schmidt, D. L. Kaplan, *J. Biomed. Mater. Res., Part B* **2011**, *99B*, 89.
[27] S. Viju, G. Thilagavathi, *Fibers Polym.* **2012**, *13*, 782.
[28] S. Nagarkar, A. Patil, A. Lele, S. Bhat, J. Bellare, R. A. Mashelkar, *Ind. Eng. Chem. Res.* **2009**, *48*, 8014.
[29] Y. F. Huang, K. Bailey, S. Wang, X. S. Feng, *React. Funct. Polym.* **2017**, *116*, 57.
[30] A. Ebrahimi, K. Sadrjavadi, M. Hajialyani, Y. Shokoohinia, A. Fattahi, *Drug Dev. Ind. Pharm.* **2018**, *44*, 199.
[31] Y. Tamada, *Biomacromolecules* **2005**, *6*, 3100.
[32] C. Chen, C. B. Cao, X. L. Ma, Y. Tang, H. S. Zhu, *Polymer* **2006**, *47*, 6322.
[33] J. Rnjak-Kovacina, L. S. Wray, K. A. Burke, T. Torregrosa, J. M. Golinski, W. W. Huang, D. L. Kaplan, *ACS Biomater. Sci. Eng.* **2015**, *1*, 260.
[34] P. P. Ma, S. Q. Gou, M. Wang, J. C. Chen, W. Hu, B. Xiao, *Macromol. Mater. Eng.* **2018**, *303*, 1700666.
[35] F. Zhang, Q. Lu, X. X. Yue, B. Q. Zuo, M. D. Qin, F. Li, D. L. Kaplan, X. G. Zhang, *Acta Biomater.* **2015**, *12*, 139.
[36] X. F. Xu, J. B. Luo, *Appl. Phys. Lett.* **2007**, *91*, 124102.

**ADVANCED
SCIENCE NEWS**

www.advancedsciencenews.com

**Macromolecular
Materials and Engineering**

www.mme-journal.de

[37] S. Mahalingam, M. Edirisinghe, *Macromol. Rapid Commun.* **2013**, *34*, 1134.

[38] X. Hong, S. Mahalingam, M. Edirisinghe, *Macromol. Mater. Eng.* **2017**, *302*, 1600564.

[39] H. H. Yuan, S. F. Zhao, H. B. Tu, B. Y. Li, Q. Li, B. Feng, H. J. Peng, Y. Z. Zhang, *J. Mater. Chem.* **2012**, *22*, 19634.

[40] B. C. Yi, H. L. Zhang, Z. P. Yu, H. H. Yuan, X. L. Wanga, Y. Z. Zhang, *J. Mater. Chem. B* **2018**, *6*, 3934.

[41] S. Koombhongse, W. X. Liu, D. H. Reneker, *J. Polym. Sci., Part B: Polym. Phys.* **2001**, *39*, 2598.

[42] U. E. Illangakoon, S. Mahalingam, P. Colombo, M. Edirisinghe, *Surf. Innovations* **2016**, *4*, 167.

[43] H. W. Ju, O. J. Lee, J. M. Lee, B. M. Moon, H. J. Park, Y. R. Park, M. C. Lee, S. H. Kim, J. R. Chao, C. S. Ki, C. H. Park, *Int. J. Biol. Macromol.* **2016**, *85*, 29.

[44] C. Liu, J. Q. Sun, M. Shao, B. Yang, *RSC Adv.* **2015**, *5*, 98553.

[45] S. W. Ha, A. E. Tonelli, S. M. Hudson, *Biomacromolecules* **2005**, *6*, 1722.

[46] T. Miyazawa, E. R. Blout, *J. Am. Chem. Soc.* **1961**, *83*, 712.

[47] S. Narayanan, M. Gokuldas, *J. Chem. Biol.* **2016**, *9*, 121.

[48] P. R. Laity, C. Holland, *Eur. Polym. J.* **2017**, *87*, 519.